JOURNAL OF GEOPHYSICAL RESEARCH, VOL. 100, NO. B8, PAGES 15,117–15,127, AUGUST 10, 1995

Comparison of along-track resolution of stacked Geosat, ERS 1, and TOPEX satellite altimeters

Mara M. Yale and David T. Sandwell

Scripps Institution of Oceanography, Institute of Geophysics and Planetary Physics, University of California, San Diego

Walter H. F. Smith

NOAA Geosciences Lab N/OES-12, National Ocean Service, Silver Spring, Maryland

Abstract. Cross-spectral analysis of repeat satellite altimeter profiles was performed to compare the along-track resolution capabilities of Geosat, ERS 1 and TOPEX data. Geophysical Data Records were edited, differentiated, low-pass-filtered, and resampled at 5 Hz. All available data were then loaded into three-dimensional files where repeat cycles were aligned along-track (62 cycles of Geosat/Exact Repeat Mission; 16 cycles of ERS 1, 35-day orbit; 73 cycles of TOPEX). The coherence versus wave number between pairs of repeat profiles was used to estimate along-track resolution for individual cycles, eight-cycle-average profiles, and 31-cycle-average profiles (Geosat and TOPEX only). Coherence, which depends on signal to noise ratio, reflects factors such as seafloor gravity amplitude, regional seafloor depth, instrument noise, oceanographic noise, and the number of cycles available for stacking (averaging). Detailed resolution analyses are presented for two areas: the equatorial Atlantic, a region with high tectonic signal and low oceanographic noise; and the South Pacific, a region with low tectonic signal and high oceanographic variability. For all three altimeters, along-track resolution is better in the equatorial Atlantic than in the South Pacific. Global maps of along-track resolution show considerable geographic variation. On average globally, the along-track resolution (0.5 coherence) of eight-cycle stacks are approximately the same, 28, 29, and 30 km for TOPEX, Geosat, and ERS 1, respectively. TOPEX 31-cycle stacks (22 km) resolve slightly shorter wavelengths than Geosat 31-cycle stacks (24 km). The stacked data, which are publicly available, will be used in future global gravity grids, and for detailed studies of mid-ocean ridge axes, fracture zones, sea mounts, and seafloor roughness.

Introduction

Recently, marine geophysics has been greatly advanced by accurate gravity maps derived from satellite altimetry data [*McAdoo and Marks*, 1992a; *Sandwell*, 1992; *Sandwell and Smith*, 1992; *Marks, et al.*, 1993]. Many applications such as charting and modeling of seamounts, mid-ocean ridges, and fractures zones require the best short-wavelength resolution possible. High-resolution gravity maps depend on both the resolution of the individual profiles and the profile spacing. Even though altimeter profile spacing is very dense in some ocean areas (currently south of 30°S), the best gravity field resolution is still slightly worse than can be obtained from modern shipboard measurements [*Neumann et al.*, 1993]. The resolution and accuracy of the individual profiles can be improved by averaging (stacking) along repeated ground tracks because the random noise component is suppressed during averaging. Stacking is possible for Geosat, ERS 1, and TOPEX since they were/are in an exact repeat orbit for at least part of their mission. Each satellite has a unique orbit that governs the spacing of the ground tracks as well as the repeat cycle duration. Optimal coverage, and thus the best two-dimensional (2-D) gravity resolution, is obtained by combining ground tracks from multiple satellites (Figure 1a). However, to intelligently combine the data from the different satellites, it is necessary to understand the resolution capabilities of each altimeter.

As in previous studies, we compare profiles that repeat to within about 1 km along the same ground track in order to assess the quality of the data [*Brammer*, 1979]. The difference between a pair of repeat profiles provides an estimate of the noise, while the coherence between repeat profiles provides a measure of the along-track resolution. Previous repeat-track analyses have shown improvement in along-track resolution with each new altimeter due to improved technology; Geos 3 ~75 km [*Brammer*, 1979; *Marks and Sailor*, 1986], Seasat ~50 km [*Marks and Sailor*, 1986; *Sailor*, 1982], Geosat individual profiles ~30 km [*Born et al.*, 1987; *Sandwell and McAdoo*, 1988], and ERS 1 individual profiles ~30 km [*McAdoo and Marks*, 1992b]. Geosat was the first altimeter to be maintained in an exact repeat orbit for a long period (~3 years) of time. Stacking many Geosat repeat profiles significantly improves accuracy and resolution so that wavelengths longer than about 20 km can be resolved [*Sandwell and McAdoo*, 1990].

In this study we assess the accuracy and resolution of both single profiles and stacked profiles from Geosat, ERS 1, and TOPEX, using the same methods so that all three altimeters can be directly compared. For each altimeter we assess the improvement gained by stacking and illustrate the many factors that control resolution including: gravity signal, oceanographic and instrument noise, ocean depth, and number of cycles available for stacking.

Paper number 95JB01308.
0148-0227/95/95JB-01308$05.00

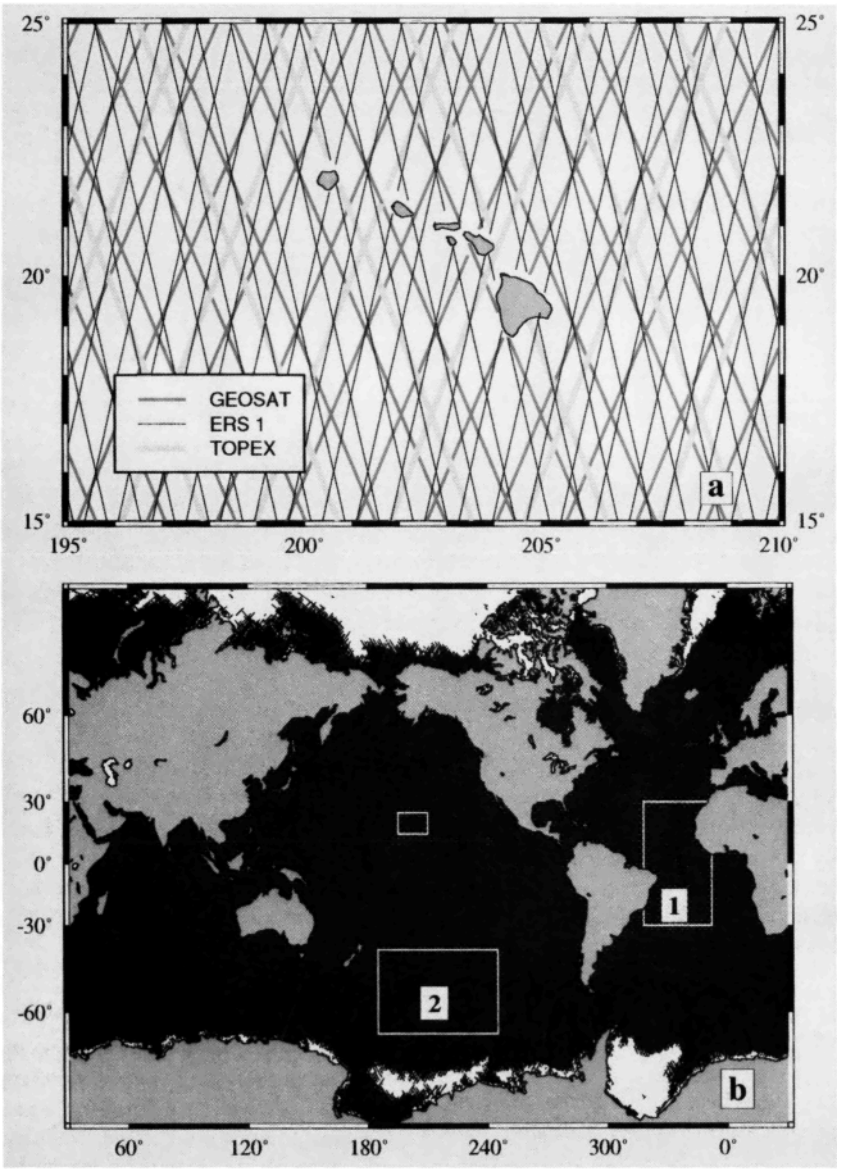

Figure 1. (a) Ground tracks for Geosat, ERS 1, and TOPEX for the region surrounding Hawaii, indicated in Figure 1b. (b) Ground tracks of ERS 1 35-day orbit. Data within regions 1 and 2 are used in the resolution analyses presented in Figure 7 and Table 3. The thick line in area 1 is the location of profiles in Figure 3 .

A major focus of our study is to understand the noise characteristics of the ERS 1 altimeter. While the TOPEX altimeter is technologically the most sophisticated and thus potentially has the best resolution, the ERS 1 35-day repeat orbit has the greatest spatial coverage and track density, making it the most valuable for detailed geophysical studies. Moreover, in April 1994, ERS 1 was placed in an orbit with a 168-day repeat cycle (16-km cross-track spacing). These new data will be the primary source of unclassified gravity information in areas north of 30°S. South of 30°S the gravity field is well constrained by declassified Geosat Geodetic Mission Data [*Marks et al.*, 1993] with ~4-km cross-track spacing. Thus the noise characteristics of ERS 1 must be well understood prior to constructing gravity grids. In particular, we wish to establish how factors such as ocean wave height influence data quality so optimal schemes for editing, filtering, and gridding the data can be designed.

The paper consists of two main parts: a data analysis section where preprocessing and stacking methods are presented and the characteristics of each data set are compared; and a resolution section that explains the procedures used and then directly compares the spectra and resolution results from analyses of all three altimeters, globally and in regions of high and low signal to noise ratios.

Data Analysis

Satellite Characteristics

The satellite characteristics are summarized in Table 1. Since these satellite altimeters orbit Earth many times each day (14.3 for Geosat and ERS 1; 12.7 for TOPEX), the duration of one repeat cycle is inversely related to the cross-track spacing at the equator. Figure 1a shows the ground tracks of all three satellites around Hawaii, illustrating the unique orbit of each satellite.

The Geosat altimeter was in a 17-day repeat cycle for 3 years; we use the first 62 cycles of Geosat Geophysical Data Record (GDR) data from November 7, 1986, to October 28, 1989

Table 1. Satellite Characteristics

	Repeat Cycle Duration, days	Cross-Track Spacing, km	Latitude Range
Geosat	17	164	±72.0°
ERS 1	35	80	±81.5°
TOPEX	10	315	±66.0°

[*Cheney et al.*, 1991]. The ERS 1 altimeter was in a 35-day repeat cycle for 17 cycles. We use cycles 2-17 of ERS 1 data from May 19, 1992, to November 30, 1993. The first 35-day cycle of ERS 1 data was not included because its ground track deviated by 2-3 km from the other 16 cycles. Ground tracks of all 35-day ERS 1 data are shown in Figure 1b. Coverage is nearly complete between ±81.5°, except in some regions of permanent sea ice (Weddell Sea, Arctic Ocean).

The TOPEX/POSEIDON mission is in a 10-day repeat cycle for the life of the satellite. TOPEX and POSEIDON are two distinct altimeters that share an antenna, so only one altimeter is operating at any time. POSEIDON is an experimental altimeter operated by Centre National d'Etude Spatiale (CNES) which was initially turned on for part of each cycle and subsequently turned on for a few entire cycles. To maintain a consistent data set related to the TOPEX altimeter, we exclude the POSEIDON data. We use cycles 1-78 of TOPEX GDR data, from September 22, 1992 to November 5, 1994, excluding POSEIDON only cycles (20, 31, 41, 55, 65).

Preprocessing

The 1 s^{-1} GDRs contain 10 sea surface height measurements, environmental corrections, and preprocessing flags. The GDRs for each satellite were edited on the basis of prior experience with Seasat data [*Marsh and Martin*, 1982] and with Geosat data [*Sandwell and McAdoo*, 1990]. Different editing criteria are applied to ERS 1 data because it is noisier than the Geosat and TOPEX data, and we show below that the noise increases as a function of significant wave height (SWH). Several of the preprocessing flags were used to eliminate 1 s^{-1} records. Data flagged as land or ice were eliminated from all three data sets. Geosat and TOPEX were both edited when the SWH was greater than 8 m or less than 0.1 m; ERS 1 was edited for SWH greater than 6 m or less than 0.01 m. Geosat and TOPEX were both edited for high and low automatic gain control (AGC); Geosat data were eliminated for AGC greater than 35 dB or less than 15 dB; TOPEX data were edited for AGC greater than 64 dB; ERS 1 GDRs did not contain AGC, and thus no AGC editing was performed on the ERS 1 data.

A procedure was used to eliminate outliers among the 10 sea surface height measurements within each 1 s^{-1} record by fitting a line to the trend of the 10 sea surface height measurements and calculating the standard deviation about this line, σ_h [*Cheney et al.*, 1991]. Geosat and TOPEX were both edited when σ_h exceeded 0.15 m; ERS 1 was edited for σ_h greater than 0.25 m.

Throughout our analysis we are interested in wavelengths shorter than 100 km where environmental corrections (tides, ionosphere, wet/dry troposphere) presumably have no signal. We tested the effect of adding corrections to the TOPEX data and found that corrected and uncorrected TOPEX deflection of the vertical data had a coherence greater than 0.5 for wavelengths longer than about 4 km, which is significantly shorter than we can resolve with the altimetry data.

A low-pass Parks-McClellan filter, designed with the MATLAB® Signal Processing Toolbox, is applied to the 10 s^{-1} data, and then the filtered data are resampled at 5 s^{-1} (Figure 2). This prestack filter is intended to suppress the high-amplitude, short-wavelength noise associated with the first difference operation that comes next. Initially, the same filter was applied to all three data sets, and it was evident that the ERS 1 data were noisier than Geosat and TOPEX data. To suppress this noise, we reprocessed the ERS 1 data with a longer filter that starts to cut off at longer wavelengths. Later, we show that these prestack filters do not attenuate signals in the band resolved by the altimeters.

After filtering, sea surface height profiles were converted to along-track sea surface slope (along-track vertical deflection) for the remainder of the analysis, according to the method of *Sandwell and McAdoo* [1990]. This conversion uses the first difference operation, which acts as a high-pass filter, amplifying short-wavelength gravity anomalies and suppressing long-wavelength orbit errors, oceanography, and environmental errors. Slope profiles of arbitrary lengths and having arbitrary data gaps can be averaged without first adjusting the DC level of each profile. Because of orbit and other long-wavelength errors, height profiles cannot be averaged this way [*Sandwell and McAdoo*, 1990]. Later, stacked slope profiles can be integrated to recover stacked height profiles with an undetermined DC level.

Stacking

After editing, filtering, and resampling, the 5 s^{-1} data from each satellite were loaded into two three-dimensional (3-D) stack files, one for ascending ground tracks and one for descending ground tracks. The characteristics of each satellite's orbit (Table 1) determine the dimensions of these files (Table 2).

Prior to loading the stack files, we developed a model (average) ground track for each satellite, based on an idealized circular orbit [*Sandwell*, 1992]. A number of representative cycles were used to constrain the important model parameters (orbit inclination and first ascending equator crossing longitude). For all three satellites the across-track deviation of the actual track from the model track was generally less than 1 km. Because the

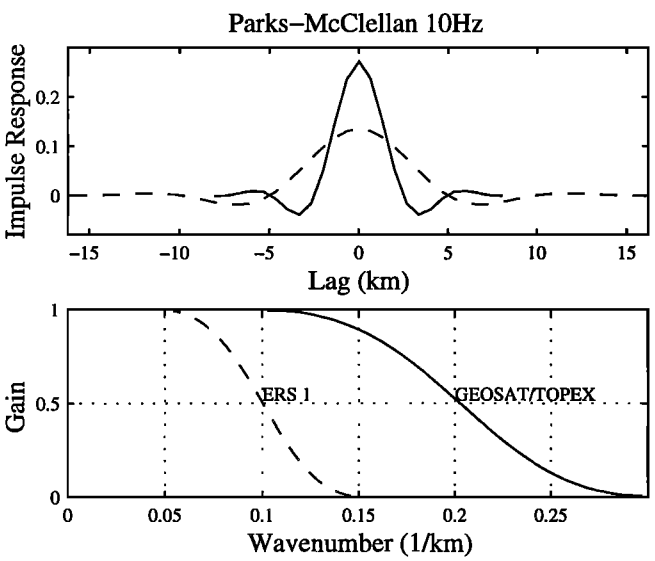

Figure 2. Filters applied to 10 Hz data (solid, Geosat and TOPEX; dashed, ERS 1). (Top) The impulse response; (bottom) the gain. ERS 1 data are noisier and thus require a longer filter (49 points versus 25 points for Geosat and TOPEX).

Table 2. Stack File Dimensions

	Number of Equator Crossings	Number of Cycles	Number of Along-Track Bins
Geosat	244	62	16000
ERS 1	501	16	17000
TOPEX	127	73	17000

idealized orbit accounts for neither the ellipticity of the actual orbit, nor the perturbing effects of Earth's oblateness, along-track deviations from the model track are sometimes larger than the along-track bin width of 1.3 km. In these cases, the model track was used to determine the approximate bin number, and then the data point was placed in the proper nearby bin. For each cycle of data, the vertical deflection and the along- and across-track deviations between the actual and model location were stored in the stack file. For ERS 1, SWH was also stored in order to assess its effect on altimeter noise. When all of the available cycles have been inserted into the stack file, we are ready to average the profiles.

The stack files provide a convenient structure for manipulating these very large data bases. To stack data, we specify which cycles to average and the range of equator crossing longitudes over which to perform the averaging. At every position along-track, we use all available cycles, among those specified, to calculate first the median deflection of the vertical and then the median absolute deviation. Points that deviate from the median by more than 3 times the median deviation are edited, following a robust method for eliminating outliers [*Rousseeuw and Leroy*, 1987]. From the remaining N points we calculate (and store) the mean and standard deviation ($N > 3$). Figure 3 illustrates the stacking of a short profile that crosses the Mid-Atlantic Ridge near the equator for all three satellites. Only eight of the available cycles are included for each satellite to show the relative quality of the data after it has been edited and filtered. (For Figure 3 only, Geosat and TOPEX individual cycles were filtered additionally before plotting so that individual cycles from each satellite have the same frequency content.) Stacked profiles based on the eight cycles shown and on all available data are also presented.

Global Characteristics of Stacks

We stacked all available ascending and descending data for each satellite and determined global measures of the number of cycles stacked and the standard deviation of each stack. The number of cycles stacked as a function of position was calculated by finding the block median of the number of cycles stacked along all the tracks that intersect each 1° Mercator cell, and then empty cells were filled by a nearest-neighbor interpolation algorithm [*Wessel and Smith*, 1991]. Figure 4 shows global maps of the number of cycles stacked for each satellite. The latitude range (Table 1) covered by Geosat and TOPEX is ice-free for at least part of the year, while the extended range of ERS 1 is limited by permanent ice coverage in some areas [*Laxon and McAdoo*, 1994]. Each map of the number of cycles stacked shows variations that depend on the altimeter. Geosat has patches of fewer cycles that are due to oscillations in the antenna direction with respect to nadir. ERS 1 has stripes of fewer cycles that are due to data loss when downloading to ground stations. TOPEX has a

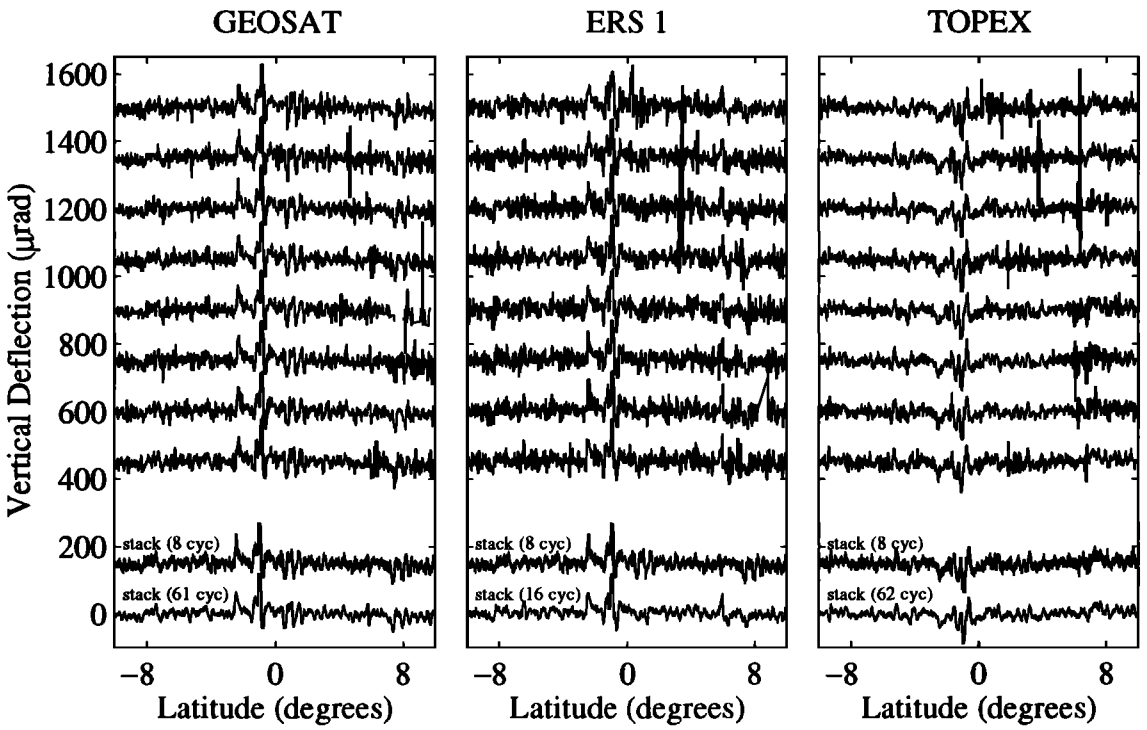

Figure 3. Individual and stacked vertical deflection profiles for a track crossing the Mid-Atlantic Ridge (thick line in area 1, Figure 1b). Only eight of the available individual cycles are shown for each satellite. TOPEX profiles have opposite sign from Geosat and ERS 1 because TOPEX was in a prograde orbit while the other satellites were in retrograde orbit. The ERS 1 stack is less well determined because ERS 1 has the fewest cycles to stack. Note that individual ERS 1 data are noisier than Geosat and TOPEX data when all contain the same frequency content.

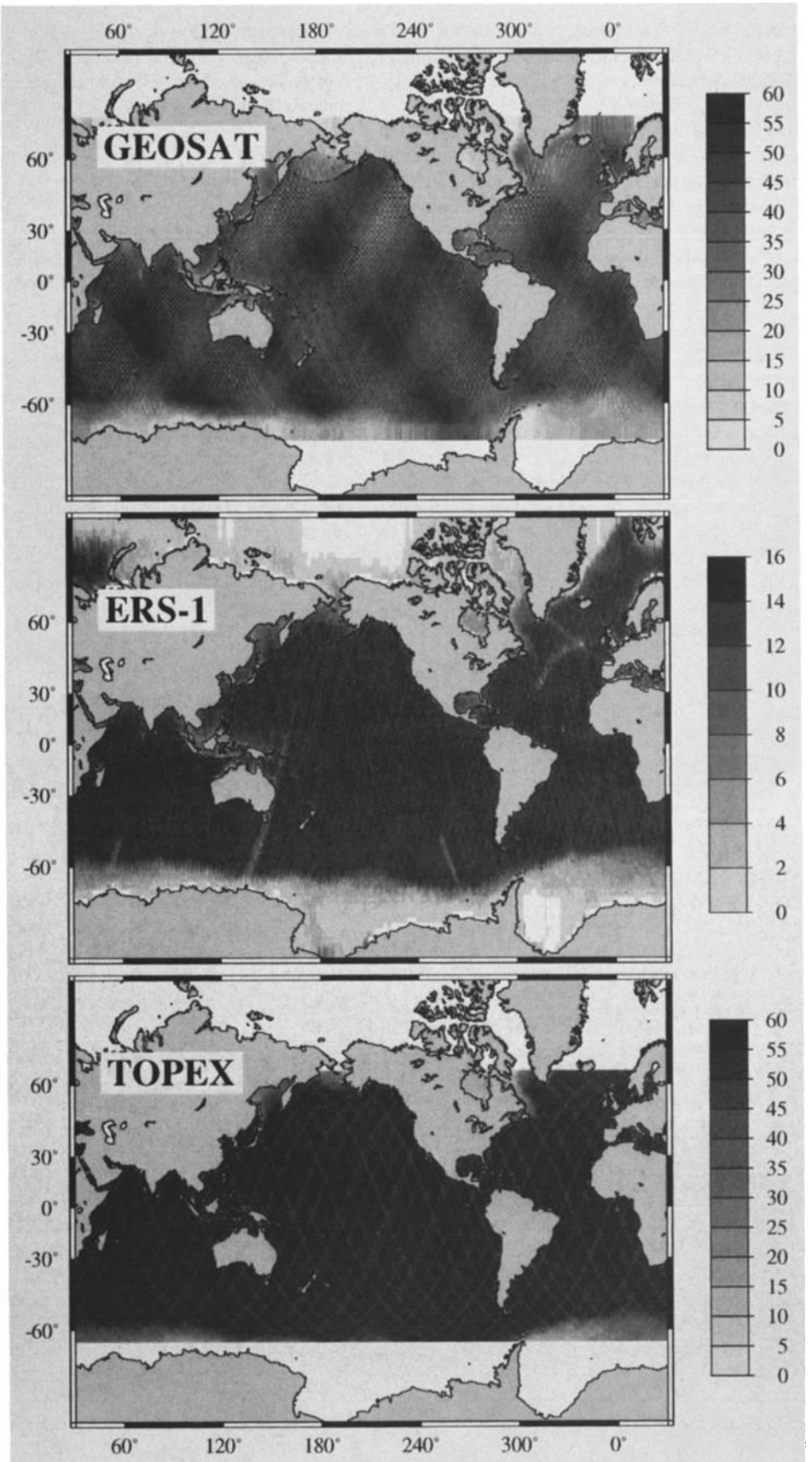

Figure 4. Number of cycles in stack for each of the satellites. Geosat, 62 possible cycles; ERS 1, 16 possible cycles; TOPEX, 62 possible cycles.

very regular pattern of stripes that look like ground tracks, where about 10 fewer cycles are stacked than in adjacent areas, due to excluding POSEIDON data from early TOPEX/POSEIDON cycles.

Global maps of the standard deviation about the stack for each satellite were made in the same way as described above for the maps of the number of cycles stacked. Figure 5 presents a global map of ERS 1 standard deviation about the stack. This map shows a very strong latitudinal dependence, with the highest standard deviation in the southern oceans, and the lowest near the equator. Maps of geographic variation in standard deviation for the other two altimeters (not shown) exhibit the same strong latitudinal dependence, while the magnitude of the standard deviation depends on how the data were filtered before stacking. The strong latitudinal dependence suggests a correlation between weather/sea state and noise in the altimeter measurements.

Global maps of average SWH (not shown) as measured by ERS 1 and other altimeters demonstrate a geographic pattern that is almost identical to the global map of geographic standard deviation of the stack shown in Figure 5. This strong apparent connection between SWH and variation of the stack motivated us to look at the deviation from the stack as a function of SWH. We stacked all available data from ERS 1 cycles 2-17 and then calculated the absolute deviation of each cycle from the stack and computed mean and median deviations in 0.05 m SWH bins. As illustrated in Figure 6, the median absolute deviation from the stack increases approximately by a factor of 2 over the range of SWH. The absolute deviation increases rapidly for SWH>6 m, and thus these data were edited.

Resolution

We follow the repeat track method for determining the resolution of altimetry data from each satellite [*Sandwell and McAdoo*, 1990]. As explained in previous studies, sea surface height measurements consist of several components, including time invariant geoid undulations and permanent long-wavelength oceanography and time-varying "noise" due to oceanographic variability, orbit error, and measurement error. Repeating altimeter profiles measure a common sea surface height signal plus "noise" which varies among repeat profiles. While ocean circulation contributes to part of the permanent sea surface topography, it consists primarily of a long-wavelength (> 1000 km), low-amplitude (< 1 μrad) signal [*Levitus*, 1982]. We are interested in resolving wavelengths shorter than 100 km; thus permanent oceanography will not limit our resolution capabilities. Our use of vertical deflection profiles instead of sea surface topography profiles changes the amplitude and shape of the power spectra but does not affect the coherence estimates [*Sandwell and McAdoo*, 1990].

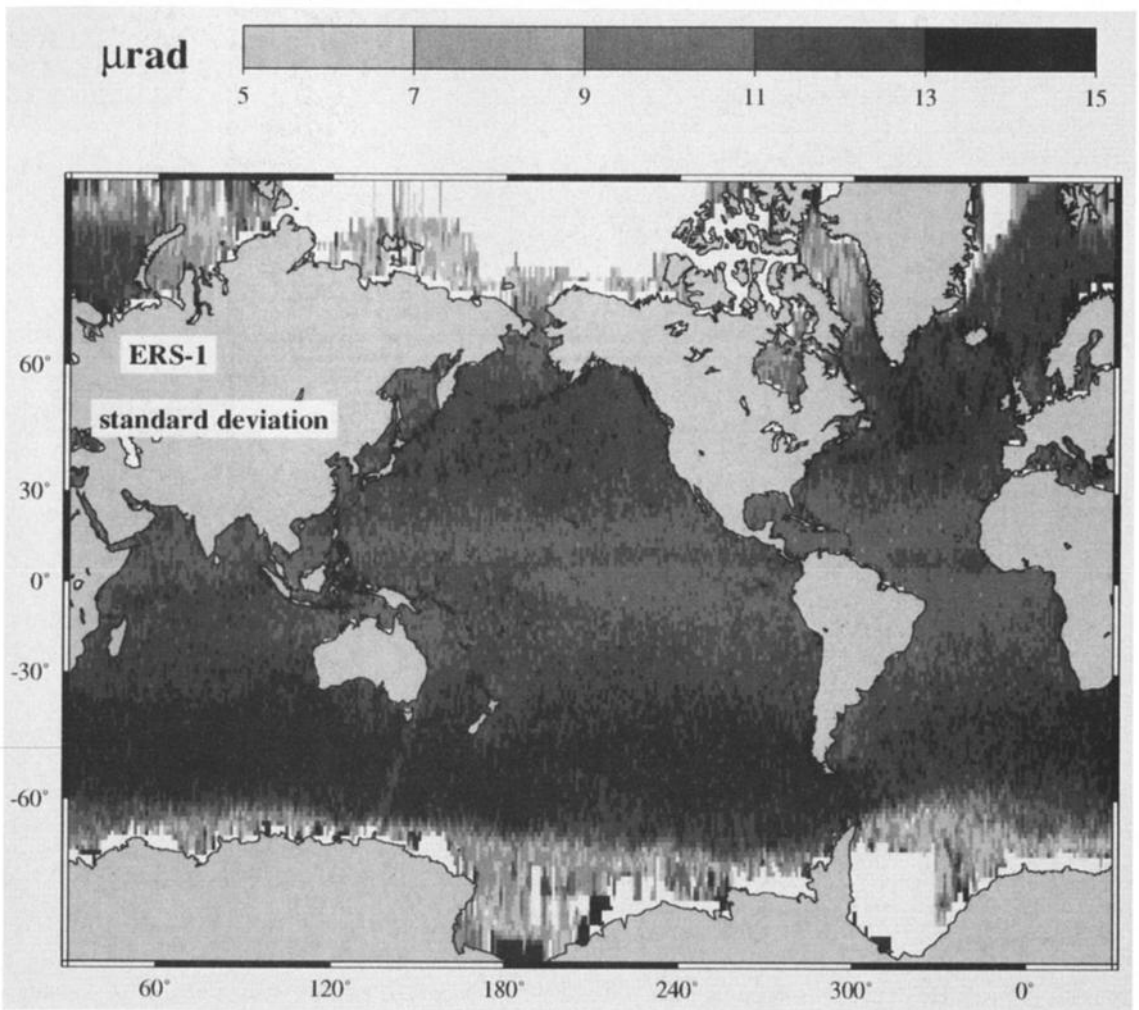

Figure 5. Standard deviation about the mean (stack) for ERS 1, reflects short-wavelength altimeter noise and altimeter noise due to high sea-state.

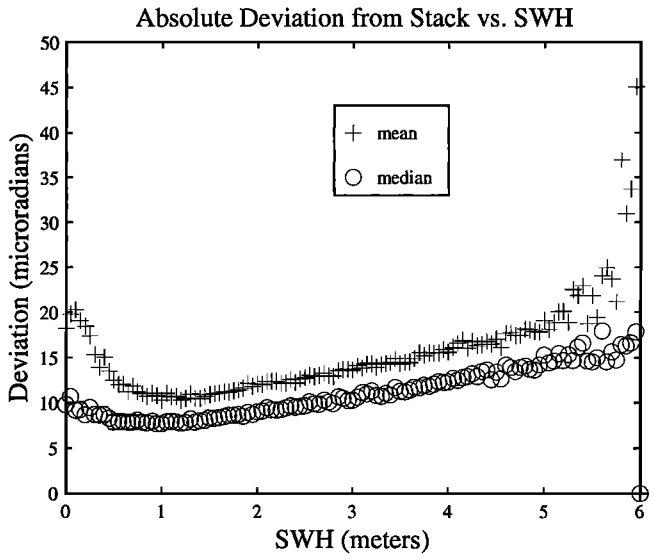

Figure 6. Absolute deviation from the stack versus significant wave height for ERS 1.

For each satellite, the repeat track method was performed on pairs of randomly selected individual cycles, and on pairs of eight-cycle stacks spanning approximately the same seasons. In addition, pairs of 31-cycle stacks of Geosat and TOPEX data were analyzed. After explaining the procedure used in all resolution analyses, detailed spectra are presented for each satellite in two areas, then results of all resolution analyses are discussed.

Data from a pair of repeat profiles are extracted from the large 3-D stack files such that corresponding points are always available, ensuring that the profiles are properly aligned, and any small data gaps are common to both profiles. We apply the *Welch* [1967] method of power and cross-spectral estimation with 50% overlap. All available profiles are split into 256 point segments (340 km for Geosat and ERS 1, 300 km for TOPEX), offset 128 points from adjacent segments. For each segment, $s_1(x)$ and $s_2(x)$ are the deflection of the vertical for the two profiles where x is the along track distance, and the noise is approximated by $d(x)=[s_1(x)-s_2(x)]/\sqrt{2}$. We first detrend and apply a Hanning window to s_1, s_2, and d before calculating the discrete Fourier transform of each. Next, we estimate the power spectral density (PSD) of s_1, s_2, and d and the cross spectrum of s_1 and s_2. Finally, power spectra and cross spectra from all available segments are averaged. The average PSDs of s_1, s_2, and d are given by

$$P_{11}=\frac{1}{N}\sum_{i=1}^{N}(S_1S_1^*)_i \qquad P_{22}=\frac{1}{N}\sum_{i=1}^{N}(S_2S_2^*)_i$$

$$P_{\text{noise}}=\frac{1}{N}\sum_{i=1}^{N}(DD^*)_i$$

respectively; and the average cross spectral density is given by

$$P_{12}=\frac{1}{N}\sum_{i=1}^{N}(S_1S_2^*)_i.$$

Capital letters denote the Fourier transform of the detrended and windowed profiles, i indicates the segment number, N is the number of segments. P_{11} and P_{22} provide a measure of the power in the signal plus the noise, while P_{noise} provides an estimate of the noise that differs between s_1 and s_2. The coherence is given by $\rho(k)=|P_{12}|^2/(P_{11}P_{22})$.

Resolution is given by the wavelength, $\lambda=1/k$ where the coherence falls to 0.5 (signal-to-noise ratio of 2.414). A model coherence is parametrically fit to the actual coherence, using the entire curve to determine the resolution [*Smith and Sandwell*, 1994]. In most of the analyses presented, resolution estimates are based on averaging the spectra from several hundred segments; however, averaging as few as 20 segments yields sufficiently smooth coherence curves for parametric fitting.

In the eight-cycle stack comparison, for ERS 1, $s_1(x)$ is an average of cycles 2-9, $s_2(x)$ is an average of cycles 10-17; for Geosat and TOPEX, $s_1(x)$ and $s_2(x)$ are averages of eight cycles that span the same period of the year as the ERS 1 eight-cycle stacks.

Area 1 and Area 2 Results

For each satellite, we use all available profiles pairs for resolution analyses in two geographic areas, area 1 in the equatorial Atlantic and area 2 in the South Pacific (Figure 1b). Profiles used run from southeast to northwest; Geosat and ERS 1 profiles are ascending as their orbits are both retrograde, while TOPEX profiles are descending as TOPEX is in a prograde orbit. Profiles in area 1 cross several prominent fracture zones and the Mid-Atlantic Ridge providing large signal, while noise is relatively low (Figure 5) and coverage is nearly complete (Figure 4) for all three satellites. All of these effects combine to make the signal to noise ratio high in area 1, and we expect the resolution in this region to represent the best possible with each altimeter. In contrast to area 1, the seafloor in area 2 is relatively smooth, and profiles cross few fracture zones, providing a relatively low tectonic signal while noise is relatively high (Figure 5), and includes a long wavelength component of oceanographic "noise" due to the variability of the Antarctic Circumpolar Current (ACC) and associated storms and waves.

The results of the resolution analyses of individual cycles and half stacks in area 1 and area 2 are presented in Figure 7. Several features of the spectra and coherence estimates are common to data from the three satellites in both areas. For both individual cycles and half stacks, P_{11} decreases as a function of increasing wave number until the signal becomes negligible with respect to the noise; the dip in power at the lowest wave numbers is due to detrending and Hanning windowing. P_{noise} increases as a function of increasing wave number. At long wavelengths, where the signal to noise ratio is high, P_{11}^{cycle} and P_{11}^{stack} are close; differences are due to data gaps in the cycle pair. At shorter wavelengths, the noise dominates the signal so P_{11} and P_{noise} are parallel and nearly coincident. One can see from Figure 7 that the reduction in the $P_{\text{noise}}^{\text{stack}}$ at high frequencies is approximately equal to the number of cycles available in each half-stack, which varies geographically and among satellites (Figure 4). Since the coherence depends on the signal to noise ratio, noise reduction due to stacking improves the resolution for all three altimeters in both areas.

The lower signal and higher noise in area 2 are clearly revealed in Figure 7. The magnitude of P_{11} in area 2 is not as high as in area 1, even at long wavelengths, due to the lack of signal. Stacking does not reduce P_{noise} by as much as in area 1, because for each satellite, the average number of cycles available for stacking in area 2 is lower than the average number available in area 1. P_{noise} for both cycle and half-stack analyses for all satellites has a bump at long wavelengths that reflects variations in the ACC between the two cycles and two half stacks. The coherence plots in area 2 reflect the component of long-wavelength

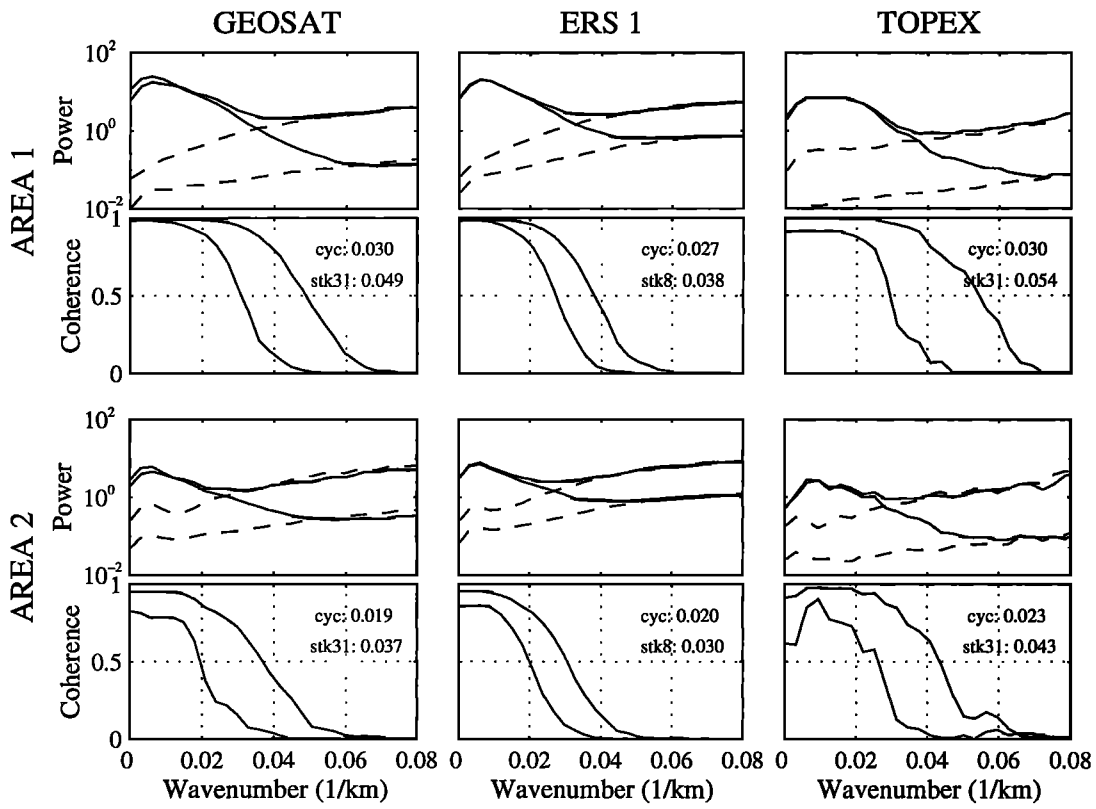

Figure 7. Power spectra and coherence curves for individual cycles and half stacks of Geosat (31 cycles), ERS 1 (8 cycles), and TOPEX (31 cycles) in area 1 (high signal, low noise) and area 2 (low signal, high noise); Figure 1b shows locations. Solid lines are power in the signal plus the noise, and dashed lines are power in the noise; the upper solid and dashed line are for an individual cycle pair, while the lower solid and dashed line are for a pair of half stacks. The wave number where the coherence is 0.5 is indicated on each coherence plot for individual cycles and half stacks.

oceanography that is contributing to the noise spectrum, as individual cycles and half stacks are significantly less coherent at the longest wavelengths than in area 1.

Quantitative evaluation of resolution is achieved by examining the coherence plots in the second and fourth rows of Figure 7. For all three satellites ρ_{stack} is greater than ρ_{cycle}. Results from areas 1 and 2 and global averages of all ascending and descending profiles from each satellite are summarized in Table 3. In addition to reflecting oceanographic variations between profiles in a pair, the resolution of individual cycles reflects the quality of the 5 s^{-1} data after filtering, while the resolution of the half stacks reflects a combination of the quality of the 5 s^{-1} data and improvement due to robust editing and averaging during stacking. When all three satellites are compared on an equal basis (eight-cycle stack), they all have approximately the same globally averaged resolution.

In all stack comparisons, TOPEX resolution is the best. TOPEX noise levels are lower for individual cycles and noise reduction is greatest for TOPEX, probably because of its uniform track density (Figure 4). TOPEX does show lower P_{11} than the other satellites in both areas, suggesting that its sparsely spaced tracks missed some high-amplitude features that Geosat and ERS 1 tracks crossed.

Global Results

As the results from area 1 and area 2 indicate substantial geographic variations in resolution, we have created global resolution maps to present the true data quality of eight-cycle stacks for ERS 1 and 31-cycle stacks for Geosat and TOPEX. For each 10°x10° geographic bin, we average the power and cross spectra for all segments centered within the bin, compute a coherence

Table 3. Summary of Along-Track Resolution Estimates

	Area 1			Area 2			Global Average		
	Cycle	Stack 8	Stack 31	Cycle	Stack 8	Stack 31	Cycle	Stack 8	Stack 31
Geosat	33	26	20	52	38	27	38	29	24
ERS 1	38	26	-	50	33	-	43	30	-
TOPEX	34	24	19	43	31	23	37	28	22

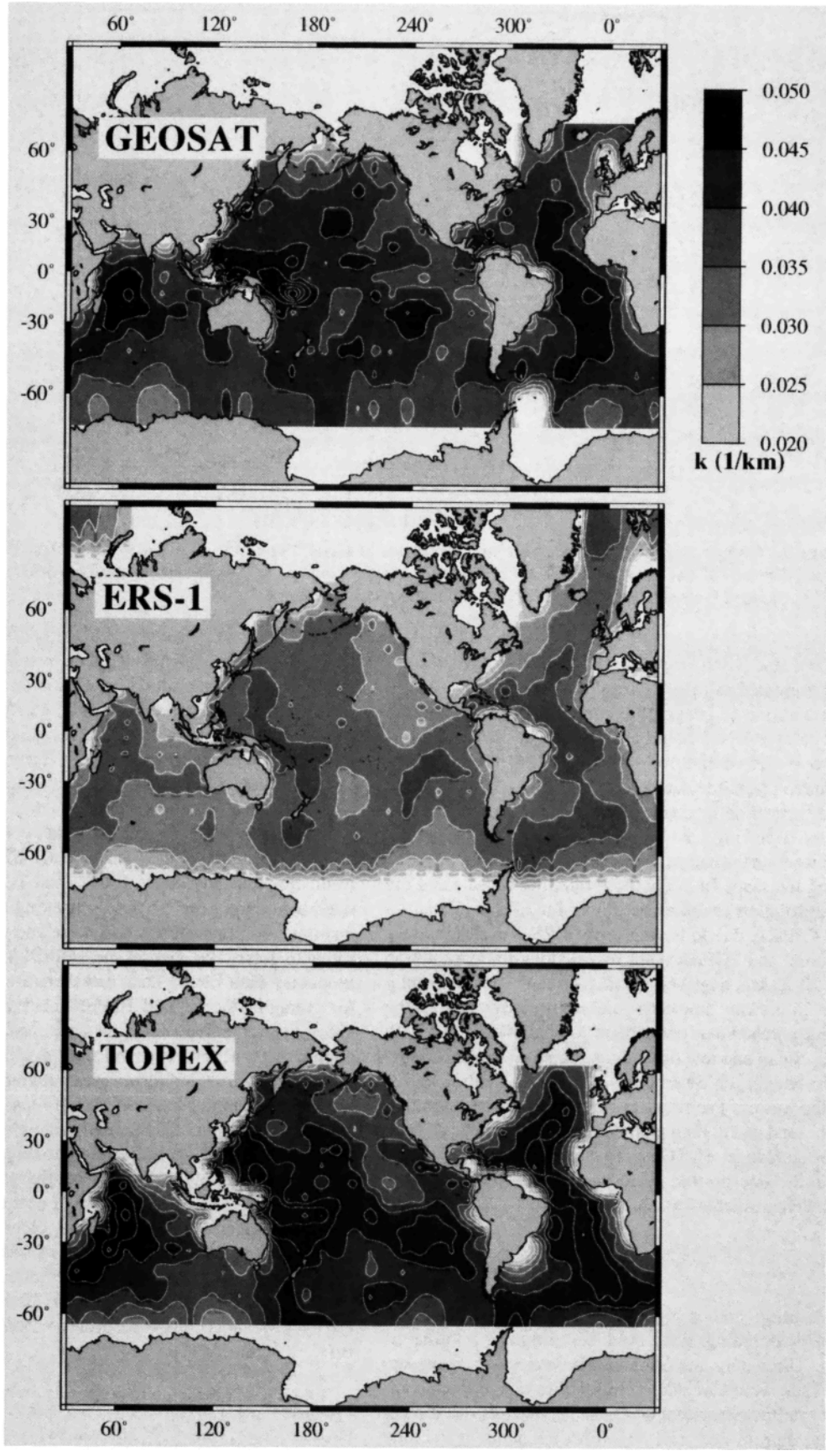

Figure 8. Resolution (0.5 coherence) as a function of geographic position. Shorter wavelengths are resolved in darker areas.

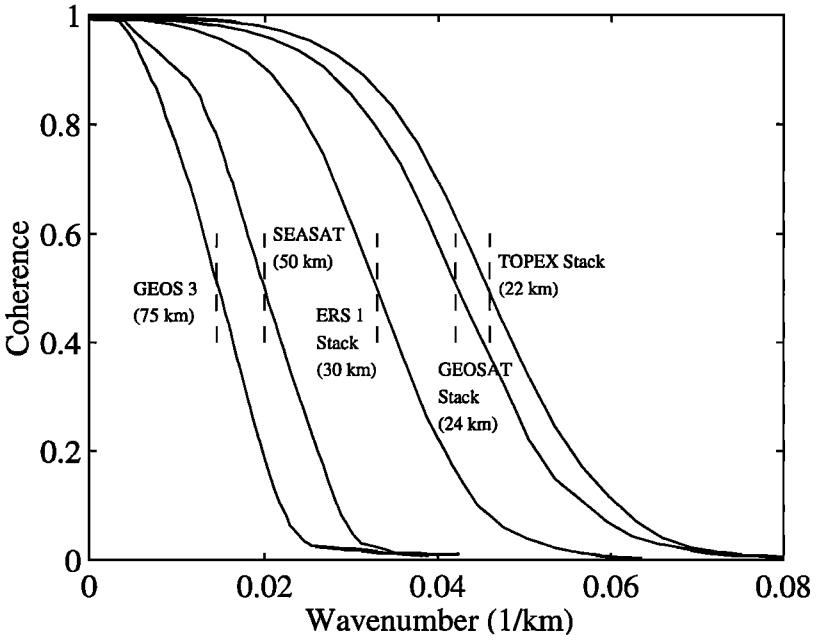

Figure 9. Comparison of coherences for single profiles of Geos 3 and Seasat, along with stacked ERS 1 (eight cycles), Geosat (31 cycles), and TOPEX (31 cycles) profiles. Geos 3 and Seasat results are from *Marks and Sailor* [1986]. Stacked Geosat, ERS 1, and TOPEX results are global averages.

curve $\rho(k)$, and find k where ρ=0.5. The resulting k values are gridded and presented as maps of resolution for each satellite in Figure 8. In addition to geographic variations in noise and the number of cycles available, regional ocean depth is also an important factor in determining resolution of altimetry data. Upward continuation from the deep seafloor (2-6 km) attenuates the amplitude of vertical deflection measured at the sea surface. For example, a signal having a 20-km wavelength is attenuated by a factor of 0.2 when the ocean depth is 5 km.

Comparing the maps from the three satellites reveals that the along-track resolution is somewhat lower for ERS 1 relative to Geosat and TOPEX, due to having fewer ERS 1 cycles to average. The Geosat and TOPEX maps reveal along-track resolution in the range 20-25 km; however, the ERS 1 map is predominantly in the range 25-33 km. For each satellite the maps have some common dark patches that correspond to shallow regions with high tectonic signal and low oceanographic noise (Figure 5): the Mid-Atlantic Ridge, the Seychelles region, the Central Indian Ridge, and the western Pacific, near New Guinea. The resolution is lowest near land and at high latitudes, where fewer cycles were available for stacking. The Geosat map has patches of higher resolution in the Pacific that correspond to the regions where more cycles were available for stacking (Figure 4).

Summary

These resolution studies highlight the many factors that are important in determining along-track resolution of satellite altimetry data. Ultimately, the resolution is determined by the signal to noise ratio which includes both satellite-independent components and satellite-dependent components. Factors that are geographically determined and satellite-independent include seafloor roughness, ocean depth, and sea surface variability. The sea surface is in a continual state of flux due to changes in seasonal weather patterns and changes in global ocean circulation. Each satellite altimeter is unique in design and therefore each has instrument specific errors including instrument noise, tracking algorithm noise, and orbit determination errors. While random instrument noise and orbit errors are not geographically dependent, we discovered that high sea state increases the uncertainty in the measurement of sea surface height. When the sea is rougher as at high latitudes, the radar pulse is scattered more, and tracking of the return pulse is less accurate.

Stacking or averaging many repeat cycles improves the resolution for all three satellite altimeters. Globally averaged coherence results for stacked Geosat, ERS 1, and TOPEX data are summarized in Figure 9 and Table 3. Stacking decreases the effect of instrument and oceanographic noise and therefore increases the signal to noise ratio. Geosat and TOPEX individual cycle data are less noisy than ERS 1 data, and there are more cycles available for averaging Geosat and TOPEX relative to ERS 1, which provides greater noise reduction and a more robust median for eliminating outliers. The number of cycles available for stacking varies by satellite and also varies geographically for each satellite, further complicating the issue of separating geographic signal and noise contributors. Globally, the along-track resolution of Geosat and TOPEX stacks are approximately the same (24 and 22 km, respectively) while the resolution of ERS 1 stacks are slightly worse (30 km). The stacked data described here provide highly accurate profiles for creating global gravity grids and for performing detailed gravity studies of fracture zones, mid-ocean ridge axes, propagating rifts, and seamounts. Global stacked deflection of the vertical profiles from Geosat (62 cycles), ERS 1 (16 cycles), and TOPEX (62 cycles) are available via anonymous ftp from arch.ucsd.edu.

Acknowledgments. ERS 1 data were provided by the French Processing and Archive Facility, IFREMER-CERSAT, BP 70, 29280 Plouzane Cedex, France, TOPEX data were provided by AVISO, NASA, and CNES. We thank John Lillibridge for providing software to convert ERS 1 Altimeter Ocean PRoduct (OPR) data to NOAA-GDR data format. This paper benefited greatly from reviews by Richard Sailor, Gregory Neumann, and an anonymous reviewer. This research was supported by the NASA Global Geophysics Program NAGW-3035.

References

Born, G. H., J. L. Mitchell ,and G. A. Heyler, Design of the Geosat exact repeat mission, *Johns Hopkins APL Tech. Dig., 8*, 260-266, 1987.

Brammer, R. F., Estimation of the ocean geoid near the Blake Escarpment using GEOS-3 satellite altimetery data, *J. Geophys. Res., 84*, 3843-3851, 1979.

Cheney, R. E., et al., *The Complete Geosat Altimeter GDR Handbook*, National Geodetic Survey, NOAA, Rockville, Md., 1991.

Laxon, S., and D. McAdoo, Arctic Ocean gravity field derived from ERS-1 satellite altimetry, *Science, 265*, 621-624, 1994.

Levitus, S., *Climatological Atlas of the World Ocean*, U.S. Dep. of Commer., Rockville, Md., 1982.

Marks, K. M., and R. V. Sailor, Comparison of GEOS-3 and Seasat altimeter resolution capabilities, *Geophys. Res. Lett., 13*, 697-700, 1986.

Marks, K. M., D. C. McAdoo, and W. H. F. Smith, Mapping the Southwest Indian Ridge with Geosat, *Eos Trans. AGU, 74*, 81, 86, 1993.

Marsh, J. G., and T. V. Martin, The Seasat altimeter mean sea surface model, *J. Geophys. Res., 87*, 3269-3280, 1982.

McAdoo, D. C., and K. M. Marks, Gravity fields of the southern ocean from Geosat data, *J. Geophys. Res., 97*, 3247-3260, 1992a.

McAdoo, D. C., and K. M. Marks, Resolving marine gravity with ERS-1 satellite altimetry, *Geophys. Res. Lett., 19*, 2271-2274, 1992b.

Neumann, G. A., D. W. Forsyth, and D. Sandwell, Comparison of marine gravity from shipboard and high-density satellite altimetry along the Mid-Atlantic Ridge, 30.5°-35.5°S, *Geophys. Res. Lett., 20*, 1639-1642, 1993.

Rousseeuw, P. W., and A. M. Leroy, *Robust Regression and Outlier Detection*, John Wiley, New York, 329 pp., 1987.

Sailor, R. V., Determination of the resolution capabilities of the Seasat radar altimeter, observations of the geoid spectrum, and detection of seamounts, report, Atlantic Sci. Corp., 1982.

Sandwell, D. T., Antarctic marine gravity field from high-density satellite altimetry, *Geophys. J. Int., 109*, 437-448, 1992.

Sandwell, D. T., and D. C. McAdoo, Marine gravity of the southern oceans and Antarctic margin from Geosat, *J. Geophys. Res., 93*, 10,389-10,396, 1988.

Sandwell, D. T., and D. C. McAdoo, High-accuracy, high-resolution gravity profiles from 2 years of the Geosat exact repeat mission, *J. Geophys. Res., 95*, 3049-3060, 1990.

Sandwell, D. T., and W. H. F. Smith, Global marine gravity from ERS-1, Geosat and Seasat reveals new tectonic fabric, *Eos Trans. AGU, 73 (44) Fall Meet. Suppl.*, 133, 1992.

Smith, W. H. F., and D. T. Sandwell, Bathymetric prediction from dense satellite altimetry and sparse shipboard bathymetry, *J. Geophys. Res., 99*, 21803-21824, 1994.

Welch, P. D., The use of fast Fourier transforms for the estimation of power spectra: a method based on time averaging over short, modified periodograms, *IEEE Trans. Audio Electroacoust., 15*, 70-73, 1967.

Wessel, P. and W. H. F. Smith, Free software helps map and display data, *Eos Trans. AGU, 72*, 441-446, 1991.

D. T. Sandwell and M. M. Yale, Scripps Institution of Oceanography, IGPP, University of California, San Diego, La Jolla, CA 92093-0225. (e-mail: myale@ucsd.edu)

W. H. F. Smith, NOAA Geosciences Lab N/OES-12, National Ocean Service, Silver Spring, MD 20910-3281.

(Received September 26, 1994; revised April 20, 1995; accepted April 24, 1995.)